NASA Technical Paper 1444

Simulated Electronic Heterodyne Recording and Processing of Pulsed-Laser Holograms

Arthur J. Decker

APRIL 1979

NASA

NASA Technical Paper 1444

Simulated Electronic Heterodyne Recording and Processing of Pulsed-Laser Holograms

Arthur J. Decker
Lewis Research Center
Cleveland, Ohio

National Aeronautics
and Space Administration

**Scientific and Technical
Information Office**

1979

SUMMARY

A method is proposed for the electronic recording of pulsed-laser holograms. By controlling the polarization sensitivity of each resolution element of the detector, an arbitrary phase can be added to the phase of the image wave. This feat is accomplished by selecting a polarization sensitivity $\sin^2[a(x,y)/2]$ in the x-direction and a polarization sensitivity $\cos^2[a(x,y)/2]$ in the y-direction, where $a(x,y)$ is the phase. The reference wave is circularly polarized, and the object wave is linearly polarized at equal angles relative to the x- and y-directions. The detector's ability to resolve the object wave is not affected by adding a phase in the manner specified.

If the hologram is scanned with an x-directed scan velocity V_x and the phase is chosen to be given by

$$a(x,y) = \delta \sin 2\pi fx$$

then a phase

$$a(t) = \delta \sin 2\pi f V_x t$$

appears in the signal generated from the electronically recorded hologram. If the frequency f is also the maximum spatial frequency in the object wave, the various terms of the hologram yield signals in nonoverlapping frequency bands. The signal corresponding to the self-interference terms of the hologram can be eliminated by bandpass filtering. The hologram constructed from the filtered signal yields nonoverlapping image waves even though the original hologram was constructed with coaxial reference and object waves.

The pulsed-laser system is based on a similar system for electronic recording and processing of continuous-wave holograms. The principle of the continuous-wave holography system for electronic recording of holograms and image processing is reviewed.

INTRODUCTION

A method has been proposed for the electronic recording and remote transmission of holograms (refs. 1 and 2). This method has the advantage that some common pro-

cedures of coherent optical processing such as cross correlation and spatial filtering are readily incorporated in the recording process.

This paper defines a system that could be used to duplicate the properties of the continuous-wave-holography system proposed in references 1 and 2 when the illumination is provided by a pulsed laser. Since the heterodyne recording essential to the concept is introduced in the spatial domain rather than in the time domain, the method is called simulated heterodyne recording. The concept is tested mathematically, and the required hologram detector (television camera tube) is defined.

The systems discussed in references 1 and 2 and in this paper can be used wherever three-dimensional image processing is required. However, the development of a pulsed-laser system is motivated by demands for optical instrumentation for use in turbomachinery research and development. The pulsed-laser technique is particularly applicable to the holographic flow-visualization methods of interest at the Lewis Research Center (refs. 3 and 4). For this reason, examples of importance in flow visualization are discussed.

This paper is both a review and extension of the work reported in an NASA-sponsored thesis (ref. 1). Before the pulsed-laser theory is developed, the material in reference 1 is reviewed by discussing the limits and restrictions on electronic recording of holograms. The analysis of an object wave for its essential information content and a method for electronic recording of holograms and image processing are presented. The paper begins with a brief section giving the reasons for recording a hologram electronically.

REASONS FOR RECORDING HOLOGRAMS ELECTRONICALLY

A primary reason for recording a hologram electronically is to permit on-line processing and analysis of an optical image. Although holography provides a "picture worth a thousand words," definitive, quantitative results in flow-field studies, for example, usually demand other coherent optical techniques such as laser Doppler velocimetry. However, with image processing and analysis, specific attributes of an image can be evaluated. For example, in principle, the electronic recording method described in this paper could be combined with a flow-visualization system to measure shock-wave orientation.

Another reason for recording a hologram electronically is to display a changing three-dimensional scene in quasi-real time. For example, three-dimensional stroboscopic imaging of an intrablade flow field during flutter in a compressor is conceivable.

Finally, of less importance in the present context is the possibility of combining electronic holography and stereoscopy for a "three-dimensional" television display.

The multiple-view holography system described in reference 2 would serve as a component of such a display.

Regardless of the reasons and methods for recording a hologram electronically, the low spatial resolution of electronic detectors (television camera tubes) is the primary constraint. That constraint is discussed in the next section.

LIMITS AND RESTRICTIONS ON ELECTRONIC RECORDING OF HOLOGRAMS

At best, electronic recording of holograms does not have sufficient resolution to allow the methods that have made dual-beam holography convenient and routine to be used. These methods have been described extensively in the literature of holography (e.g., refs. 5 and 6). Because of the completeness of the literature, only a brief discussion of dual-beam holography is presented here to show where the resolution restriction asserts itself.

The dual-beam hologram was proposed by Gabor in 1948 (ref. 7). In recording the hologram, two monochromatic beams of light are incident on a plane called the recording plane, as shown in figure 1(a). The first beam, called the object wave, is represented by the complex phasor $U(x, y, z)$. The second beam, called the reference wave $U_R(x, y, z)$, has the same polarization as the object wave and is coherent with it. The two beams interfere at the hologram-recording plane to yield an intensity that is proportional to

$$I(x, y, z) = |U_R(x, y, z)|^2 + |U(x, y, z)|^2 + U_R^*(x, y, z)U(x, y, z) + U_R(x, y, z)U^*(x, y, z) \tag{1}$$

where the asterisk denotes complex conjugation. A so-called linear recording is made such that the amplitude transmittance $T(x, y, z)$ of the recording is directly proportional to the intensity

$$T(x, y, z) = \gamma I(x, y, z) \tag{2}$$

The reconstruction procedure shown in figure 1(b) consists of illuminating the recording with a replica of the reference wave $U_R(x, y, z)$. Four waves are reconstructed and constitute the four diffraction orders of a linearly recorded dual-beam hologram. At the hologram-recording plane, these waves, in order of the terms in equation (1), are

$$\gamma |U_R(x, y, z)|^2 U_R(x, y, z)$$

$$\gamma |U(x, y, z)|^2 U_R(x, y, z)$$

$$\gamma |U_R(x, y, z)|^2 U(x, y, z)$$

$$\gamma U_R(x, y, z) U_R(x, y, z) U^*(x, y, z)$$

Only the third wave is proportional to the original object wave. The first wave is proportional to the original reference wave. The second wave arises from a term where the object wave has interfered with itself. The fourth wave, if the object wave originated from a three-dimensional object, forms a real image.

The resolution requirement of the recording process is determined from the Fourier transformation of the third term in equation (1). At the hologram-recording plane, where z is constant, the spatial transforms of the reference and object waves are defined by

$$\left.\begin{aligned} O(f_x, f_y) &= \iint_{-\infty}^{\infty} U(x, y) e^{-j2\pi f_x x - j2\pi f_y y}\, dx\, dy \\ R^*(f_x, f_y) &= \iint_{-\infty}^{\infty} U_R^*(x, y) e^{-j2\pi f_x x - j2\pi f_y y}\, dx\, dy \end{aligned}\right\} \tag{3}$$

Both U and U_R are assumed to be essentially nonzero over the hologram segment only. All interpretations are simple if U and U_R are imagined to be composed of plane waves

$$O(f_x, f_y) e^{j2\pi f_x x + j2\pi f_y y}$$

$$R(f_x, f_y) e^{j2\pi f_x x + j2\pi f_y y}$$

where

$$2\pi f_x = k \cos \varphi_x$$

$$2\pi f_y = k \cos \varphi_y$$

where $k = 2\pi/\lambda$ is the wave number and φ_x and φ_y are the angles between the propagation vectors and the x- and y-axes, respectively.

The transform $\mathcal{T}\{I_3\}$ of the third term I_3 in equation (1) is given by

$$\mathcal{T}\{I_3\} = O(f_x, f_y) \otimes R^*(f_x, f_y) = \int\int_{-\infty}^{\infty} O(f_x - f'_x,\ f_y - f'_y)\, R^*(f'_x, f'_y)\, df'_x\, df'_y \tag{4}$$

where the symbol $\otimes$ denotes the convolution operation defined in equation (4). If O and R are approximately band limited, the following conclusions are easily drawn by considering the limiting plane waves. Only the f_x variation is considered since the same conclusions hold for the f_y variation. The spectra O and R are considered to be symmetrically distributed about f_{ox} and f_{rx} and to have half-widths Δf_{ox} and Δf_{rx}, respectively. Then $\mathcal{T}\{I_3\}$ is distributed in the interval

$$\left[f_{ox} - f_{rx} - (\Delta f_{ox} + \Delta f_{rx}),\ f_{ox} - f_{rx} + (\Delta f_{ox} + \Delta f_{rx})\right]$$

Clearly, the maximum frequency that must be recorded is minimized at $\Delta f_{ox} + \Delta f_{rx}$ if $f_{ox} = f_{rx}$. Then, the reference and object beams are coaxial. If the beams are not coaxial, the maximum frequency that must be recorded is increased by the difference

$$|f_{ox} - f_{rx}| = \frac{k}{2\pi} |\cos \varphi_{ox} - \cos \varphi_{rx}| \tag{5}$$

The virtual-image axis is determined by

$$2\pi f_{ox} = k \cos \varphi_{ox} \tag{6}$$

and the real-image axis is determined by

$$2\pi(2f_{rx} - f_{ox}) = k \cos \varphi_{Rx} \tag{7}$$

where φ_{Rx} is the angle of the real-image axis. The axes of the real-image and virtual-image waves are coaxial if $f_{rx} = f_{ox}$.

Finally, the first two terms of equation (1) can be transformed. The transformation of the first term is distributed in the interval $(-2\ \Delta f_{rx},\ 2\ \Delta f_{rx})$ and the transformation of the second term is distributed in the interval $(-2\ \Delta f_{ox},\ 2\ \Delta f_{ox})$. Generally, $\Delta f_{ox} > \Delta f_{rx}$, so that upon reconstruction it can be shown that self-interference terms produce radiation in the spatial-frequency interval

$$\left[f_{rx} - 2\ \Delta f_{ox} - \Delta f_{rx},\ f_{rx} + 2\ \Delta f_{ox} + \Delta f_{rx}\right]$$

But the term I_3 yields radiation in the interval

$$\left[f_{ox} - \Delta f_{ox} - 2\,\Delta f_{rx},\ f_{ox} + \Delta f_{ox} + 2\,\Delta f_{rx}\right]$$

If $f_{rx} = f_{ox}$, it is clear that the self-interference terms yield a larger beam divergence than do the image-wave terms. If $f_{ox} = f_{rx}$ and Δf_{rx} is small, the maximum frequency that must be resolved is determined by the half-bandwidth of the object-wave transform.

We now have the information necessary to define the resolution required by any hologram-recording process. The use of coaxial object and reference waves minimizes the maximum frequency that must be recorded and, thereby, minimizes the resolution requirement of the recording medium. Unfortunately, then the diffraction orders overlap. The signal-to-noise ratio of the reconstruction is reduced enormously: Only one order contains the original object wave, and three of the orders are simply noise.

At the expense of a greatly increased resolution requirement, Leith and Upatnieks proposed their famous solution of this overlap problem (ref. 8). If the object wave is distributed about $f_{ox} = 0$ (beam axis perpendicular to recording plane), choosing the reference-beam angle φ_{rx} such that

$$f_{rx} \geq 3\,\Delta f_{ox} \tag{8}$$

assures separation of the orders. The Fourier transform of equation (1) is shown schematically in figure 2(a) for such a choice. Clearly, the object-wave term is in an entirely different spatial band than are the other terms. Most practical applications of holography employ the off-axis reference-beam method of Leith and Upatnieks. This method makes holography convenient and routine.

The extreme difficulty of using the Leith-Upatnieks method with electronic recording is readily shown by an example. Consider a 525-line television camera tube with an 18-millimeter diagonal. The tube conveniently has the same number of resolution elements in the horizontal and vertical directions. For a 3:4 aspect ratio, the horizontal resolution f in sinusoidal cycles per millimeter falls in the ordinary photographic resolution range, about 18 per millimeter. The reference frequency must be centered at $3\,\Delta f_{ox}$ (fig. 2(a)) and the camera tube must resolve

$$4\,\Delta f_{ox} = f \tag{9}$$

Hence, the maximum recordable object-wave frequency Δf_{ox} is about 4.5 per millimeter, a value probably not worth the effort.

If the hologram is recorded electronically, there is approximately a one-to-one correspondence between horizontal spatial frequency and temporal frequency. With filtering, it is possible to use a single sideband of an image term to construct an adequate hologram for a symmetrical object wave. As shown in figure 2(b), the reference wave must be centered at $2\,\Delta f_{ox}$ and the hologram need resolve only $3\,\Delta f_{ox}$. The maximum detail is now 33 percent of the available resolution, or 6 per millimeter, a value still not worth the effort. Clearly, another solution of the overlap-of-orders problem must be found if electronic recording is to be used.

In addition to not having enough resolution for the off-axis reference-beam method, an electronic detector may not have enough resolution for all object-wave half-widths Δf_{ox}. A multiple-view holography method such as the method of reference 2 is a solution of this problem. However, a large object-wave bandwidth is usually a matter of convenience rather than necessity. In fact, in flow-visualization applications, the bandwidth can be set fairly arbitrarily. The information content and bandwidth of an object wave are discussed in the next section.

INFORMATION CONTENT AND BANDWIDTH OF AN OBJECT WAVE

The principles that govern how well a holographic system records and replicates an object wave are the principles of optical imaging discussed extensively by Born and Wolf (ref. 9). The modeling of an object wave such that the essential information can be isolated is discussed in reference 1. Hence, only the results are stated here and supported by some examples. The object-wave-processing ability of a holographic system can be summarized in a few paragraphs.

Electronic holography is quite capable of recording the macroscopic patterns of surface and volume that identify an object. These patterns have transforms within the resolution range of the detector. Electronic holography is also capable of defining an object wave in three dimensions. This property is determined by the depth of focus in the image space and the depth of field in the object space of an optical system. These depths are determined by the numerical aperture of the recording method. In electronic holography, the numerical aperture is the sine of the half-angle of the largest resolvable pencil of rays from a point source.

The adequacy of an electronic holography system is really challenged by physiological rather than physical requirements. Wide-angle viewing of an extended object requires a large object-wave bandwidth. Stereoscopic viewing requires that each point on an object direct light to both eyes. These requirements are met by a diffuser or a diffusing surface whose microstructure increases the object-wave bandwidth. These statements are amplified in the following paragraphs.

As shown in reference 1, the transform of the object wave from a surface can be expressed by the equation

$$O(f_x, f_y) = \left[\mathcal{F}\{I(x', y', z')\} \otimes \mathcal{F}\{T(x', y', z')\}\right] e^{-j\pi\lambda(z-d)\left(f_x^2+f_y^2\right)} \tag{10}$$

where d is the distance from the recording plane to a local origin of the surface, $I(x', y', z')$ is an equivalent illumination function, and $T(x', y', z')$ is an equivalent transmittance or reflectance of the surface. The function $T(x', y', z')$ contains the macroscopic variations in phase and magnitude that define the surface pattern. The maximum spatial frequency of the object wave is obtained by adding the maximum frequency contained in the illumination $I(x', y', z')$ to the maximum frequency contained in the equivalent transmittance $T(x', y', z')$.

In most cases, $T(x', y', z')$ will not have enough bandwidth to use the full numerical aperture of an electronic detector. Then a diffuser must be employed to increase the bandwidth of $I(x', y', z')$ for minimum depth of field. In fact, a diffuser should be used with a bandwidth determined by the full numerical aperture of the detector. Because sum and difference frequencies are involved, the information in $T(x', y', z')$ is still retained. As explained by Leith and Upatnieks (ref. 10), the required dynamic range of the recording process is reduced by using a diffuser. Liu and Gallagher (ref. 11) explain how to design an optimum diffuser for an object.

These comments are reinforced by a simple, yet relevant, example diagrammed in figure 3. A discontinuity in refractive index (a shock wave) is illuminated with a plane wave. A hologram is recorded. Because the machinery causing the shock wave moves, the shock wave rotates through a small angle $\Delta\theta_s$. A second hologram is recorded. Because linear recording is used, the effect is the same as if the two holograms had been recorded simultaneously and the two refracted waves were propagating simultaneously from the vicinity of the shock wave.

The figure exaggerates angles for clarity. The refracted waves occupy a spatial band that is easily determined from Snell's law of refraction. For the refraction from position 1,

$$\frac{\cos\theta_s}{\cos(\theta_s + \theta_1)} = \frac{n_2}{n_1} \tag{11}$$

where the refractive indices on the consecutive sides of the shock wave are designated n_1 and n_2. For the refraction from position 2,

$$\frac{\cos(\theta_s - \Delta\theta_s)}{\cos(\theta_s - \Delta\theta_s + \theta_2)} = \frac{n_2}{n_1} \tag{12}$$

Because the example refers to a gas, θ_1 and θ_2 are small angles. By retaining only first-order terms in small angles in equations (11) and (12), the band occupied by the two refracted waves is given by

$$2\,\Delta f_{ox} = \frac{\theta_2 - \theta_1}{\lambda} = \frac{\Delta\theta_s}{\lambda}\,\frac{n_2 - n_1}{n_2} \tag{13}$$

A large value for the refractive index change is given by

$$n_2 - n_1 = 0.0003$$

Also, n_2 is approximately 1.0. If the wavelength λ of a helium-neon laser is chosen as 0.633 micrometer, the spatial bandwidth of the equivalent transmittance of the doubly exposed shock wave is given by

$$\frac{2\,\Delta f_{ox}}{\Delta\theta_s} = \frac{1/2}{\text{mm}\cdot\text{rad}}$$

Clearly, a diffuser is needed to fill the entire numerical aperture of a television camera tube with a resolution of 18 per millimeter.

Two additional simple calculations illustrate the other points made in this section. From reference 1, the depth of field δ of the recording method is given by

$$\delta = \frac{1.03}{f^2\lambda} \tag{14}$$

where f is the frequency resolution of the recording method. When λ is 0.633 micrometer and f is 18 per millimeter, the depth of field is 5 millimeters. A 2.5-centimeter-deep object could be resolved into about 6 longitudinal stations for true three-dimensional recording.

Finally, suppose that we wish to use stereoscopic vision with an 18-per-millimeter recording. For an object point midway between the eyes, the minimum viewing distance S is given by

$$S = \frac{D}{2\lambda f} \tag{15}$$

where D is the pupil separation. When D is 6 centimeters, λ is 0.633 micrometer, and f is 18 per millimeter, S is equal to 2.6 meters. Clearly, at that distance there would be little feeling of depth for a 2.5-centimeter-deep object. Methods for resolving this problem are discussed in references 1 and 2.

Provided that the full resolution of a detector is available for recording the object wave, electronic recording of holograms is quite reasonable. A method for making the full resolution available is discussed in the next section.

ELECTRONIC RECORDING OF HOLOGRAMS

The main body of the analysis in this section is presented in references 1 and 2. The main purpose of this paper is to emulate in the spatial domain the time-domain processing discussed in these references. The processing technique can then be used with pulsed-laser holography. Hence, the time-domain analysis is repeated for quick reference. This section shows how to record a hologram that does not have the object-wave self-interference term and that also separates the virtual and real image-wave terms. Other sometimes-difficult-to-implement methods of electronic holography are described in references 12 to 14 and mentioned in references 1 and 2.

An arrangement for electronically recording low-resolution holograms of semitransparent objects is shown in figure 4. A similar arrangement for recording holograms of reflecting objects is shown in figure 5. This paper is concerned with semitransparent objects of the type found in flow visualization; hence, figure 4 is primarily of interest.

The key elements in figure 4 are

(1) A beam splitter to combine the object and reference waves coaxially for low-resolution recording

(2) An electro-optic phase modulator (ref. 15) for varying the phase of the reference wave in time

(3) A continuous-wave laser

(4) An image dissector or any other scanned detector with an instantaneous response, as opposed to an integrating detector such as a vidicon

The arrangement of figure 4 will implement the method known as heterodyne recording. In heterodyne recording, the reference wave contains different time-frequency components than does the object wave. Each component interferes with the object wave to generate a time-varying interference pattern. The pattern varies at a frequency equal to the difference between the frequencies of the object- and reference-wave components. An instantaneous detector is required to record the pattern at a position at a particular instant of time.

In heterodyne recording, the hologram must be scanned electronically. Scanning is discussed, for example, by Macovski (ref. 16). The object and reference waves will interfere to form a changing intensity pattern $I(x, y, t)$. A scanning aperture $S(x, y)$ is moved over this pattern at horizontal and vertical velocities V_x and V_y. The instantaneous power from the scanning aperture P_i is calculated by integrating $I(x, y, t)$ weighted by the scanning aperture centered at its instantaneous position $x_c(t)$, $y_c(t)$.

$$P_i\left[x_c(t), y_c(t), t\right] = \int\int_{-\infty}^{\infty} dx\, dy\, S(x - x_c, y - y_c) I(x, y, t) \tag{16}$$

The finite response of the system is represented by a detector impulse-response function $h_o(t - t')$ that is nonzero only for $t \geq t'$. The electrical signal upon scanning is given by

$$f(t) = \int_{-\infty}^{t} h_o(t - t') P_i\left[x_c(t'), y_c(t'), t'\right] dt' \tag{17}$$

Because of the need to scan back and forth in a raster, $x_c(t)$ and $y_c(t)$ are not simple functions of time. However, on a scan line

$$\left.\begin{aligned} \frac{dx_c(t)}{dt} &= V_x \\ \frac{dy_c(t)}{dt} &= V_y \end{aligned}\right\} \tag{18}$$

The finite duration of a scan line and the finite duration of a frame increase the signal bandwidth slightly in comparison with the contribution of $I(x, y, t)$. In television practice, the frame is scanned in two fields to eliminate visual flicker. These effects add nothing to the analysis and are not considered further.

The inverse process of writing a hologram pattern from a signal is similar. Suppose that the signal after processing, transmission, and reception is $f_R(t)$. A writing intensity is generated that is given by

$$I_w(t') = \int_{-\infty}^{t'} f_R(t'') h_w(t' - t'') dt'' \tag{19}$$

The intensity is applied to a writing aperture $W(x,y)$, where the writing aperture is scanned at horizontal and vertical velocities V'_x and V'_y. At time t, the writing aperture is centered at $x'_c(t), y'_c(t)$. The exposure at a point x,y is given by

$$E(x,y) = \int_{-\infty}^{\infty} W\left[x - x'_c(t), y - y'_c(t)\right] I_w(t)dt \tag{20}$$

The only other comment that will be made about writing a hologram in this manner is that, if $V'_x \neq V_x$ and $V'_y \neq V_y$, a scale transformation will result.

The detector response $h_o(t)$ and the scanning aperture $S(x,y)$ are chosen to be delta functions:

$$h_o(t) = \delta(t) \tag{21}$$

$$S(x,y) = \delta(x)\delta(y) \tag{22}$$

This simplification is harmless if $S(x,y)$ is narrow enough to resolve the desired object detail and if $h_o(t)$ is narrow enough to pass a faithful replica of the scanned, time-varying intensity pattern. On a scan line beginning at $0, y_o$

$$\left.\begin{aligned} x_c(t) &= V_x t \\ y_c(t) &= y_o + V_y t \end{aligned}\right\} \tag{23}$$

The signal is then given by

$$f(t) = I(V_x t, y_o + V_y t, t) \tag{24}$$

and is determined directly from the intensity distribution in the hologram pattern.

Heterodyne recording is now easily explained. The object and reference waves are written in real notation as

$$\left.\begin{aligned} U(x,y) &= O(x,y)\cos[\omega t - \varphi(x,y)] \\ U_R(x,y) &= s(x,y)\cos\left[\omega t - r(x,y) + a(t) + \delta \sin \omega_H t\right] \end{aligned}\right\} \tag{25}$$

where the circular frequency of the light wave is denoted by ω and a phase modulation term $a(t) + \delta \sin \omega_H t$ has been introduced in the phase of the reference wave. Note that source retardation is negligible at the frequencies of interest. The reference wave can be phase modulated by using an electro-optic modulator. Temporarily, we equate

a(t) to zero so that the remaining phase modulation $\delta \sin \omega_H t$ depends on a depth-of-modulation parameter or modulation index δ and a heterodyne circular frequency ω_H.

By performing square-law detection to eliminate the dependence on ω and by using the well-known Bessel function series (ref. 17)

$$\left.\begin{aligned} \cos(\delta \sin \omega_H t) &= J_0(\delta) + 2 \sum_{\ell=1}^{\infty} J_{2\ell}(\delta) \cos 2\ell\omega_H t \\ \sin(\delta \sin \omega_H t) &= 2 \sum_{\ell=0}^{\infty} J_{2\ell+1}(\delta) \sin\left[(2\ell + 1)\omega_H t\right] \end{aligned}\right\} \tag{26}$$

the hologram intensity is proportional to

$$\begin{aligned} I(x,y,t) = {} & O^2(x,y) + s^2(x,y) + 2s(x,y)O(x,y) \cos[\varphi(x,y) - r(x,y)] \\ & \times \left[J_0(\delta) + 2 \sum_{\ell=1}^{\infty} J_{2\ell}(\delta) \cos 2\ell\omega_H t\right] \\ & - 2s(x,y)O(x,y) \sin[\varphi(x,y) - r(x,y)] \left\{\sum_{\ell=0}^{\infty} 2J_{2\ell+1}(\delta) \sin\left[(2\ell + 1)\omega_H t\right]\right\} \end{aligned} \tag{27}$$

Note that the time variation contributed by scanning and the time variation contributed by phase modulation are quite independent. The depth-of-modulation parameter can be used to emphasize different harmonics. For example, by setting δ equal to 2.62, the first five orders of Bessel functions are

$$\left.\begin{aligned} J_0(\delta) &= -0.106 \\ J_1(\delta) &= 0.465 \\ J_2(\delta) &= 0.461 \\ J_3(\delta) &= 0.239 \\ J_4(\delta) &= 0.0863 \end{aligned}\right\} \tag{28}$$

The first four terms in harmonics of ω_H are

$$\left.\begin{aligned} I_0(x,y,t) &= O^2(x,y) + s^2(x,y) - 0.212\, s(x,y)O(x,y)\cos[\varphi(x,y) - r(x,y)] \\ I_1(x,y,t) &= -1.86\, s(x,y)O(x,y)\sin[\varphi(x,y) - r(x,y)]\sin\omega_H t \\ I_2(x,y,t) &= 1.84\, s(x,y)O(x,y)\cos[\varphi(x,y) - r(x,y)]\cos 2\omega_H t \\ I_3(x,y,t) &= -0.956\, s(x,y)O(x,y)\sin[\varphi(x,y) - r(x,y)]\sin 3\omega_H t \end{aligned}\right\} \quad (29)$$

Each of these terms contains a cross-interference term suitable for reconstructing the image waves. Because of the simple manner in which scanning affects the time dependence through equation (24), each spatial-frequency pair f_x, f_y contributes a corresponding time-frequency component

$$f_t = V_x f_x + V_y f_y \quad (30)$$

Generally,

$$\left.\begin{aligned} &\frac{V_y}{V_x} \ll 1 \\ &\text{and} \\ &f_t \approx V_x f_x \end{aligned}\right\} \quad (31)$$

In that case, each time-frequency component generated by scanning corresponds to a unique x-directed spatial-frequency component.

By the proper choice of ω_H, each of the terms I_0, I_1, . . . can be placed in nonoverlapping bands and selected independently by band-pass filtering in the time domain. However, only I_0 contains the self-interference terms; hence, the elimination of I_0 completes the heterodyne recording process and solves the overlap problem.

If Δf_{rx} is negligible, the requirement for unqualified separation of all signals I_0, I_1, . . . is given by

$$f_H \geq 3V_x \Delta f_{ox} \quad (32)$$

For the equality sign, the bands for the first three signals (fig. 6) are

I_0:

$$\left[0,\ 2V_x\,\Delta f_{ox}\right]$$

I_1:

$$\left[2V_x\,\Delta f_{ox},\ 4V_x\,\Delta f_{ox}\right]$$

I_2:

$$\left[5V_x\,\Delta f_{ox},\ 7V_x\,\Delta f_{ox}\right]$$

If we assume that the scanning aperture does not resolve spatial frequencies greater than Δf_{ox}, the requirement on f_H can be relaxed somewhat. The separation requirement is

$$f_H \geq 2V_x\,\Delta f_{ox} \tag{33}$$

When the equality sign is selected, the bands are shown in figure 7 and are

I_0:

$$\left[0,\ V_x\,\Delta f_{ox}\right]$$

I_1:

$$\left[V_x\,\Delta f_{ox},\ 3V_x\,\Delta f_{ox}\right]$$

I_2:

$$\left[3V_x\,\Delta f_{ox},\ 5V_x\,\Delta f_{ox}\right]$$

If f_H is decreased further, the bands overlap and the hologram constructed from such a signal yields overlapping multiple images. Equation (33) sets the lower limit on f_H in order to avoid overlap.

The signals I_1 and I_2 carry the complete hologram in either sideband. For the equality sign in equation (33), the lower sidebands are

I_1:

$$\left[V_x\,\Delta f_{ox},\ 2V_x\,\Delta f_{ox}\right]$$

I_2:

$$\left[3V_x\,\Delta f_{ox},\ 4V_x\,\Delta f_{ox}\right]$$

The corresponding signals are

$$\left.\begin{aligned} I_1 &= 0.93\ s(x,y)O(x,y)\cos\left[\varphi(x,y) - r(x,y) - \omega_H t\right] \\ I_2 &= 0.92\ s(x,y)O(x,y)\cos\left[\varphi(x,y) - r(x,y) - 2\omega_H t\right] \end{aligned}\right\} \tag{34}$$

The substitution $x = V_x t$ has not been made explicitly.

A hologram produced from either signal in equation (34) is an equivalent of an off-axis reference-beam hologram. For simplicity, choose the writing aperture $W(x,y)$ and the writing response function $h_w(t)$ to be delta functions. If $V'_x = V_x$ and $V'_y = V_y$, the hologram generated from I_1 contains the term

$$I_1(x,y) = 0.93\ s(x,y)O(x,y)\cos\left[\varphi(x,y) - r(x,y) - \frac{\omega_H x}{V_x}\right] \tag{35}$$

This hologram is equivalent to a hologram recorded with a reference beam that is off axis at an angle θ given by

$$\sin\theta = \frac{f_H}{V_x}\lambda \geq 2\,\Delta f_{ox}\lambda \tag{36}$$

The axis of the real-image wave appears at θ_{ri}, where

$$\sin\theta_{ri} = \frac{2f_H}{V_x}\lambda \geq 4\,\Delta f_{ox}\lambda \tag{37}$$

The virtual- and real-image waves are in the spatial-frequency bands $[-\Delta f_{ox},\ \Delta f_{ox}]$ and $[3\,\Delta f_{ox},\ 5\,\Delta f_{ox}]$, respectively. These results are summarized by figure 8.

The following properties are needed to test the feasibility of heterodyne recording. If $V_x\,\Delta f_{ox} \approx 4\times10^6$ hertz, as with standard television (ref. 18),

$$f_H \geq 2V_x\,\Delta f_{ox} = 8\times10^6 \text{ hertz}$$

For equality, I_1 is in the single sideband [4×10^6 Hz, 8×10^6 Hz] and I_2 is in the single sideband [12×10^6 Hz, 16×10^6 Hz]. Of course, the required frequencies and bandwidths are reduced if V_x is reduced. The scanned system must have an $h_o(t)$ narrow enough to respond to the maximum frequency. A television camera tube with the required properties is the image dissector tube, which is essentially a photomultiplier in which an electron image is formed and scanned over a pinhole aperture. Finally,

to record the intensity given in equation (35), we still need a medium with resolution $3\,\Delta f_{ox}$. If the detector has a resolution of 18 per millimeter, the final recording medium should resolve 54 per millimeter. If resolution is a problem, f_H can be reduced to f'_H after electronic recording so that

$$\sin\theta = \frac{f'_H}{V_x}\lambda \geq \Delta f_{ox}\lambda$$

$$\sin\theta_{ri} = \frac{2f'_H}{V_x}\lambda \geq 2\,\Delta f_{ox}\lambda$$

The reconstructed waves are barely separated, but the required resolution is only 36 per millimeter.

Although phase modulation is an extremely convenient method for heterodyne recording of holograms and a good solution of the overlap problem, there is at least one other method of heterodyne recording in the literature (ref. 14). The unique feature of phase modulation is that it simplifies image processing. This property must also be emulated by a system that records pulsed-laser holograms. The use of continuous-wave electronic holography for image processing is discussed in the next section.

IMAGE PROCESSING

Methods of image processing as a means for extracting data from film are reviewed in reference 19. The theory of optical processing in continuous-wave electronic holography requires a rather lengthy development, as presented in reference 1. A brief summary of the development appears in reference 2. However, since we eventually wish to show that the same operations can be effected in pulsed-laser holography, another brief summary is included here.

Essentially, two operations are required in coherent optical processing: filtering of the spatial spectrum for image enhancement and cross correlation of the input wave for pattern recognition. Optically, both operations are performed by inserting a mask (spatial filter) in the spatial-frequency domain. In cross correlation the input wave is typically Fourier transformed by means of a lens (ref. 6) and then passed through a mask that has an amplitude transmittance proportional to the Fourier transform of the second wave. A second lens is used to invert the transform to complete the cross-correlation operation. This process is summarized in figure 9.

The best-known application of the process shown in figure 9 is matched filtering. The mask is chosen to be the complex conjugate of the Fourier transform of the input

wave. Phase is canceled, and the output can be focused to a minimum-diameter spot by the second lens to show that the input is matched to the mask. For filter masks that can be expressed in the form

$$H(x, y) = e^{ja(x, y)} \tag{38}$$

the entire process can be performed without lenses with heterodyne recording. The key operation is the multiplication of a hologram by an arbitrary phase distribution.

If the phase modulation again contains $a(t)$, the first three terms of the interference pattern are

$$\left.\begin{aligned} I_0 &= s^2(x, y) + O^2(x, y) + 2J_0(\delta)s(x, y)O(x, y)\cos[\varphi(x, y) - r(x, y) + a(t)] \\ I_1 &= -4J_1(\delta)s(x, y)O(x, y)\sin[\varphi(x, y) - r(x, y) + a(t)]\sin\omega_H t \\ I_2 &= 4J_2(\delta)s(x, y)O(x, y)\cos[\varphi(x, y) - r(x, y) + a(t)]\cos 2\omega_H t \end{aligned}\right\} \tag{39}$$

The time t is associated with the position $x_c(t)$, $y_c(t)$ of the center of the scanning aperture. As in the description of heterodyne recording, a delta-function scanning aperture is chosen, and the scan line is to be horizontal. On a scan line,

$$y = y_o$$

$$t = \frac{x}{V_x}$$

and $a(t)$ is mapped into a function $a(x, y)$. Hence, each cross-interference term in the hologram is multiplied by an aribtrary phase factor $e^{\pm ja(x, y)}$.

However, the presence of $a(t)$ in the phase increases the bandwidth with each signal. Either the spatial-frequency content of the object wave must be decreased accordingly, or the scan velocity V_x must be reduced. The required restrictions are determined as follows. The phase is to be controllable within the range $-\pi \le a(t) \le \pi$. The maximum frequency at which the phase is likely to be varied is $V_x f_{xm}$, where $f_{xm} = \Delta f_{ox}$ is the maximum x-directed spatial frequency in the object wave. Hence, the worst-case time variation of $a(t)$ is given by

$$a(t) = \pi \sin 2\pi V_x f_{xm} t \tag{40}$$

With the modulation index π, at least the first four harmonics of $V_x f_{xm}$ must be counted on. Hence, a sideband must cover at least the range $5V_x f_{xm}$. If the full resolution of the detector is to be used, the scan velocity must be reduced by at least a

factor of 5. Interestingly, if the full resolution of the detector is used, the hologram finally constructed from the signal will represent an image wave of higher spatial frequency than could originally have been recorded. At this point, the system necessary to perform spatial filtering is available.

In spatial filtering, an amplitude distribution

$$b(x_o, y_o) = O(x_o, y_o)e^{j\varphi(x_o, y_o)} \tag{41}$$

in an input plane is first Fourier transformed. A slight modification of the system shown in figure 4 will perform this transformation without lenses. The modified system is shown in figure 10. As derived in reference 1, the output signal is given by

$$I_1 = \int\int_{-\infty}^{\infty} O(x_o, y_o) \cos\left[\varphi(x_o, y_o) - \frac{2\pi}{\lambda s}(xx_o + yy_o) + a(t) - \omega_H t\right] dx_o\, dy_o \tag{42}$$

where the correspondence between position and time is not shown explicitly. After it is constructed from the signal, the hologram is illuminated by an axially directed plane wave. The axes of the real- and virtual-image waves are directed at angles $\pm\sin^{-1} f_H\lambda/V_x$, respectively.

The transformation must still be inverted by a lens. A better method is to modify the system depicted in figure 10 to use hologram-scale transformations. The scale of a hologram is easily changed in electronic recording by making the scan velocity V'_x, V'_y used to write the hologram different from the scan velocity V_x, V_y used to read the hologram. If the hologram has a transmittance $T(x,y)$ before the scale change, it will have a transmittance $T(x/a, y/a)$ after the scale change, where the scale parameter a is given by

$$a = \frac{V_{x'}}{V_x} = \frac{V_{y'}}{V_y} \tag{43}$$

As shown in references 1 and 2, choosing an a of 0.707 makes it possible to use a diverging spherical wave to illuminate the object. The virtual image is placed at infinity and the real image is used as the output. The actual output for an input $b(x_o, y_o)$ is given by

$$I_R = b^*\left(0.707\ x - \frac{f_H kS}{V_x}, 0.707\ y\right) \otimes h^*(0.707\ x, 0.707\ y) \tag{44}$$

where h is the inverse transform of the mask H. The output I_R is the complex conjugate of the desired output and appears magnified and off axis. However, none of these features is a problem in an application such as matched filtering.

The recording and reconstruction processes are shown schematically in figure 11. The input transparency is placed at a distance S from the image dissector. The reference wave originates at a distance 2S from the image dissector. The illumination of the subject transparency originates at a distance S in front of the transparency. Reconstruction is accomplished with a beam converging to a distance 2S in back of the hologram. The output appears at a distance S in back of the hologram but off axis.

Lensless transformations and scaling can be performed with any electronic recording method. The key feature in using phase modulation with continuous-wave holography is that the phase $\delta \sin \omega_H t + a(t)$ can be inserted without reducing the available spatial resolution of the detector. The emulation of this method in pulsed-laser holography is the subject of the next section.

ELECTRONIC RECORDING OF PULSED-LASER HOLOGRAMS

In continuous-wave electronic holography, information is, in effect, stored in both the spatial domain and the time domain. As demonstrated, the entire spatial resolution of the detector is then available for recording the object wave. In pulsed-laser holography, the time domain is no longer available. The only alternative is to try to control another attribute of the electric field. Optical holograms ordinarily record the magnitude and phase of a single polarization of the electric field. Hence, varying the polarization is another way to code information and is adopted as the approach here. The objective is to generate a signal like the signal represented by equation (39). Then, the overlap problem is solved, and an arbitrary phase modulation has been applied. Furthermore, the entire spatial resolution of the detector must be available for resolving the object wave.

To implement the system for pulsed-laser holography, the detector must have the following properties:

(1) Because of the short duration of the pulse (20 nsec from a Q-switched ruby laser), the detector must be an integrating one. Most television camera tubes have this property.

(2) The polarization sensitivity of the detector must be controllable, one resolution element at a time. That is, given two orthogonal directions on the resolution element, the sensitivities to intensity of light polarized in those two directions must be independently controllable.

Unlike the continuous-wave case, where the image dissector has the desired properties, there seems to be no detector that has a polarization sensitivity controllable on an element-by-element basis. There are physical phenomena, however, that might be exploited to realize this property. These phenomena include variable dichroism in crystals (ref. 20) and magnetic domain control (ref. 21).

An experimental arrangement would consist of modifying a few items in figure 10. The required modifications are as follows:

(1) The image dissector is replaced with a detector of the type previously defined.

(2) The reference wave is circularly polarized by inserting a quarter-wave plate in the reference-wave path. (The laser emits a linearly polarized beam.)

(3) The object wave is linearly polarized at equal angles with respect to the control directions.

(4) The phase modulator is replaced by a "black box" for controlling polarization sensitivity.

Maintaining a linear polarization of the object wave is relatively easy in flow-visualization applications. A diffuser can be constructed that does not depolarize the illuminating beam, and the weakly refracting object does not disturb the polarization.

The mathematical proof of this system is presented here. The circularly polarized reference wave has the form

$$\overline{U}_r = s_x \cos(\omega t - r)\hat{i} + s_y \sin(\omega t - r)\hat{j} \tag{45}$$

where $\hat{i}$ and $\hat{j}$ are unit vectors along the x- and y-directions, respectively. The vector $\overline{U}_r$ and the scalars s_x, s_y, and r are possibly functions of position. Note that $s_x = s_y$; however, subscripts are retained to identify the polarization. A real notation will be used throughout this section; hence, ω is the circular frequency of the light. The linearly polarized object wave is given by

$$\overline{U}_o = o_x \cos(\omega t - \varphi)\hat{i} + o_y \cos(\omega t - \varphi)\hat{j} \tag{46}$$

Again, $o_x = o_y$ although subscripts are retained to identify polarization. The vector $\overline{U}_o$ and the scalars o_x, o_y, and φ are possibly functions of position. The square-law detectable intensity I is given by

$$I = \frac{1}{\tau} \int_{\substack{\text{Integral over many} \\ \text{optical cycles}}} \left(U_o^2 + U_r^2 + 2\overline{U}_o\overline{U}_r\right)dt$$

$$= \frac{o_x^2 + s_x^2}{2} + s_x o_x \cos(\varphi - r) + \frac{o_y^2 + s_y^2}{2} + s_y o_y \sin(\varphi - r) \tag{47}$$

where τ is the integration time.

A major requirement is that the polarization sensitivity not increase the resolution requirement of the detector: The entire spatial resolution is to be available for resolving the object wave. To check that this requirement is met, let the detector consist of an array of square apertures. Weight each aperture with a polarization sensitivity $\sin^2[a(X, Y)/2]$ in the x-direction and a polarization sensitivity $\cos^2[a(X, Y)/2]$ in the y-direction, where the coordinate of the center of the aperture is denoted by X, Y. The aperture is assumed to have a side length L. The signal read from a resolution element during a scan is proportional to the expression

$$S = o^2 + s^2 + \left(\frac{1}{L^2}\right)\sin^2\left[\frac{a(X, Y)}{2}\right]\int_{X-\frac{L}{2}}^{X+\frac{L}{2}} dx \int_{Y-\frac{L}{2}}^{Y+\frac{L}{2}} dy \; so \cos(\varphi - r)$$

$$+ \left(\frac{1}{L^2}\right)\cos^2\left[\frac{a(X, Y)}{2}\right]\int_{X-\frac{L}{2}}^{X+\frac{L}{2}} dx \int_{Y-\frac{L}{2}}^{Y+\frac{L}{2}} dy \; so \sin(\varphi - r) \qquad (48)$$

The subscripts have been dropped from s and o. Here, the aperture must be small enough to reproduce the maximum-frequency component in $\sin^2[a(X, Y)/2]$ by sampling.

The aperture must also be small enough to resolve the maximum-frequency component in $so \cos(\varphi - r)$.

$$\frac{1}{L^2}\int_{X-\frac{L}{2}}^{X+\frac{L}{2}} dx \int_{Y-\frac{L}{2}}^{Y+\frac{L}{2}} dy \; so \cos(\varphi - r) \approx so \cos(\varphi - r)_{X, Y} \qquad (49)$$

where the subscript X, Y denotes evaluation of the function at the center of the aperture. The point to note is that the entire resolution of the detector is available for resolving the object wave. The resolution conditions apply separately to the two factors in the cross-interference terms of equation (48). A detector to resolve the pattern

$$\sin^2\left[\frac{a(x, y)}{2}\right] so \cos(\varphi - r)$$

directly would need a resolution equal to the sum of the maximum frequencies in the two factors.

Noting that the resolution requirement is satisfied and keeping that requirement in mind, for simplicity assume a delta-function aperture. The signal read during a scan is then proportional to

$$S = o^2 + s^2 + \sin^2\left[\frac{a(x,y)}{2}\right] so\cos(\varphi - r) + \cos^2\left[\frac{a(x,y)}{2}\right] so\sin(\varphi - r) \tag{50}$$

The use of squared trigonometric functions has ensured that the self-interference terms $o^2 + s^2$ are not multiplied by a sensitivity factor. The signal can be written as

$$S = o^2 + s^2 + \frac{so}{2}\cos(\varphi - r) + \frac{so}{2}\sin(\varphi - r)$$

$$- \cos a(x,y)\frac{so}{2}\cos(\varphi - r) + \cos a(x,y)\frac{so}{2}\sin(\varphi - r) \tag{51}$$

The last two terms in equation (51) will yield reconstructed waves containing an arbitrary phase in the manner of equation (39). We show that the phase can be used to place these terms in bands that do not overlap the self-interference terms.

Select $a(x,y) = \delta \sin 2\pi fx$, where f is the maximum spatial frequency that can be sampled by the aperture. As discussed, the frequency f will be the maximum spatial frequency that can be resolved in the object wave. For an x-directed scan velocity V_x, the corresponding time signal from the cross-interference terms containing an arbitrary phase factor is

$$S = -\cos(\delta \sin 2\pi f V_x t)s(V_x t, y)o(V_x t, y)\left[\cos\ \varphi(V_x t, y) - r(V_x t, y)\right]$$

$$+ \cos(\delta \sin 2\pi f V_x t)s(V_x t, y)o(V_x t, y)\sin\left[\varphi(V_x t, y) - r(V_x t, y)\right] \tag{52}$$

After the usual expansion, the first three terms are

$$\left.\begin{aligned} S_0 &= -J_0(\delta)s(V_x t, y)o(V_x t, y)\ [\cos(\varphi - r) - \sin(\varphi - r)] \\ S_1 &= -2J_2(\delta)s(V_x t, y)o(V_x t, y)\cos(4\pi f V_x t)\ [\cos(\varphi - r) - \sin(\varphi - r)] \\ S_2 &= -2J_4(\delta)s(V_x t, y)o(V_x t, y)\cos(8\pi f V_x t)\ [\cos(\varphi - r) - \sin(\varphi - r)] \\ &\ \ \vdots \end{aligned}\right\} \tag{53}$$

In keeping with the term "heterodyne," we define

$$\omega_H = 2\pi f V_x$$

We also recognize the correspondence between time and position by writing $V_x t$ as x. The terms become

$$\left.\begin{aligned} S_0 &= -J_0(\delta)s(x,y)o(x,y)\,[\cos(\varphi - r) - \sin(\varphi - r)] \\ S_1 &= -2J_2(\delta)s(x,y)o(x,y)\,[\cos(\varphi - r) - \sin(\varphi - r)]\cos 2\omega_H t \\ S_2 &= -2J_4(\delta)s(x,y)o(x,y)\,[\cos(\varphi - r) - \sin(\varphi - r)]\cos 4\omega_H t \end{aligned}\right\} \qquad (54)$$

These terms are similar to those in equation (27) or (29) with the following exceptions:

(1) Odd multiples of ω_H are missing.

(2) The $\cos(\varphi - r)$ and $\sin(\varphi - r)$ are both present, although this feature does not affect the spectrum or the reconstruction.

The various terms of the spectrum occupy the following bands (fig. 12):

(1) Self-interference terms occupy the band $(0, 2fV_x)$. However, the detector does not resolve spatial frequencies greater than f so that the actual signal corresponding to these terms is in the band $(0, fV_x)$.

(2) The S_0 term occupies the band $(0, fV_x)$.

(3) The S_n terms occupy the bands

S_1:

$$(fV_x,\ 3fV_x)$$

S_2:

$$(3fV_x,\ 5fV_x)$$

.
.
.

Clearly, the terms multiplied by $\cos 2N\omega_H t$, where N is an integer, do not overlap the self-interference terms or cross-interference terms in the time domain and can be selected by filtering.

At this point, the pulsed-laser system has been proven. It is interesting to note that the criterion for bands not overlapping is that

$$f_H \geq \Delta f_{ox} V_x \tag{55}$$

However, if $f = \Delta f_{ox}$ is the maximum resolvable spatial frequency, the equality sign must apply:

$$f_H = \Delta f_{ox} V_x \tag{56}$$

In continuous-wave holography, the criterion according to equation (33) was

$$f_H \geq 2 \Delta f_{ox} V_x \tag{57}$$

That criterion cannot be satisfied in the pulsed-laser case. The missing odd multiples of ω_H make electronic recording of pulsed-laser holograms feasible. To implement image processing, the arbitrary phase distribution $a(x, y)$ is applied by varying the polarization sensitivity.

CONCLUDING REMARKS

For the benefit of the cursory reader who might be interested in recording holograms electronically, a few concluding remarks are in order. These conclusions are easily drawn from the theory or the examples.

Electronic recording of holograms is intended primarily as an information-processing method, not as a viewing method. For a single recording, the width of a nearby object is limited to the width of the detector. Even then, the eyes must be at a large distance from the hologram for stereoscopic viewing. However, the development of a display for three-dimensional viewing is not entirely precluded. There are electronic plotters that will display orders-of-magnitude more resolution elements than can be resolved by a detector at one time. This resource can be used to make viewing easier in the following ways: A wide-angle view can be recorded as a series of views. An array of detectors can be used to record an extended object. To implement stereoscopic viewing, an object wave can be multiplied by a random-phase diffuser during recording, or the image-wave terms can be separated from the self-interference terms by filtering, stored in a computer memory, and then multiplied by the random-phase diffuser.

The development of a system for electronically recording a hologram really consists of several projects: The feasibility of a detection method must be demonstrated. An appropriate detector must be developed or found in the pulsed-laser case. The value of the detection method in image processing must be proven. Attempts to write

a hologram from a signal result in another set of projects. However, the variety of materials for storing holograms and the higher resolution attainable in writing a hologram from a signal should make these projects easier.

Lewis Research Center,
National Aeronautics and Space Administration,
Cleveland, Ohio, November 30, 1978,
505-04.

APPENDIX - SYMBOLS

a	scale parameter
$a(t)$	arbitrary-phase modulation
$a(x, y)$	arbitrary phase to be added to phase of object wave
$b(x_o, y_o)$	amplitude distribution at an input plane of an image-processing system
D	pupil separation
d	distance from recording plane to local origin of surface
E	exposure
f, f_x, f_y, f_{xm}	spatial frequency
f_H	heterodyne frequency
f_{ox}	central spatial frequency of object wave
Δf_{ox}	half-bandwidth of object wave
f_{rx}	central spatial frequency of reference wave
Δf_{rx}	half-bandwidth of reference wave
f_t	time frequency
$f(t)$	electrical signal
$f_R(t)$	signal following processing, transmission, and reception
$H(x, y)$	amplitude transmittance of filter
h	inverse transform of filter mask (impulse response function of an optical system)
$h_o(t)$	detector impulse response function
$h_w(t)$	impulse response function for writing a hologram
$I(x, y, z), I(x, y, t)$	intensity
I_w	writing intensity
$\hat{i}$	unit vector in x-direction
J_n	Bessel function of first kind, n^{th} order
j	imaginary designator
$\hat{j}$	unit vector in y-direction

k	wave number
L	length of square scanning aperture
n_1, n_2	refractive index
$O(f_x, f_y)$	Fourier transform of object-wave amplitude
o_x, o_y	magnitudes of x- and y-components of object wave
$o(x, y)$	magnitude of object wave
P_i	instantaneous power from scanning aperture
$R(f_x, f_y)$	Fourier transform of reference-wave amplitude
$r(x, y)$	phase of reference wave
S	signal or distance from hologram
$S(x, y)$	scanning aperture
s_x, s_y	magnitudes of x- and y-components of reference wave
$s(x, y)$	magnitude of reference wave
$T(x, y, z)$	amplitude transmittance
$\mathcal{T}$	Fourier transform
t	time
$U(x, y, z)$	phasor representing an object-wave amplitude
$U_R(x, y, z)$	phasor representing an image-wave amplitude
$\overline{U}_o$	real vector amplitude of object wave
$\overline{U}_R$	real vector amplitude of reference wave
V_x, V_y	scan velocities in x- and y-directions
$W(x, y)$	writing aperture
x, y, z	Cartesian coordinates
$x_c(t), y_c(t)$	instantaneous position of center of scanning aperture
γ	proportionality constant
δ	either depth-of-modulation parameter or depth of field
$\delta(x), \delta(y), \delta(t)$	Dirac delta function
θ	angle of reconstructed virtual-image wave relative to optical axis
θ_{ri}	angle of reconstructed real-image wave relative to optical axis

θ_s angle of a shock wave

$\Delta\theta_s$ angle of rotation of a shock wave

θ_1, θ_2 angles of refraction

λ wavelength

φ_{ox} angle of object-wave axis relative to x-direction

φ_{Rx} angle of real-image axis

φ_{rx} angle of reference-wave axis relative to x-direction

φ_x angle of propagation of plane wave relative to x-axis

φ_y angle of propagation of plane wave relative to y-axis

$\varphi(x, y)$ phase of object wave

ω circular frequency of light

ω_H heterodyne circular frequency

Superscripts:

* complex conjugate

$'$ equivalent

REFERENCES

1. Decker, A. J.: Electronic Heterodyne Recording and Processing of Optical Holograms Using Phase Modulated Reference Waves. Ph.D. Thesis, Case Western Reserve Univ., Cleveland, Ohio, 1977.

2. Decker, A. J.; Pao, Yoh-Han; and Claspy, P. C.: Electronic Heterodyne Recording and Processing of Optical Holograms Using Phase Modulated Reference Waves. Appl. Opt., vol. 17, Mar. 1978, pp. 917-921.

3. Wuerker, R. F.; Kobayashi, R. J.; Heflinger, L. O.; and Ware, T. C.: Application of Holography to Flow Visualization Within Rotating Compressor Blade Row. (AIRESEARCH-73-9489, AiResearch Mfg. Co.; NASA Contract NAS3-15336.) NASA CR-121264, 1974.

4. Heflinger, L. O.; Wuerker, R. F.; and Brooks, R. E.: Holographic Interferometry. J. Appl. Phys., vol. 37, no. 2, Feb. 1966, pp. 642-649.

5. Collier, Robert J.; Burckhardt, Christoph B.; and Lin, Lawrence H.: Optical Holography. Academic Press, 1971.

6. Goodman, Joseph W.: Introduction to Fourier Optics. McGraw-Hill Book Co., Inc., 1968.

7. Gabor, D.: A New Microscopic Principle. Nature (London), vol. 161, May 15, 1948, pp. 777-778.

8. Leith, Emmett N.; and Upatnieks, Juris: Reconstructed Wavefronts and Communication Theory. J. Opt. Soc. Am., vol. 52, no. 10, Oct. 1962, pp. 1123-1130.

9. Born, Max; and Wolf, Emil: Principles of Optics. Third Rev. ed., Pergamon Press, 1965.

10. Leith, Emmett N.; and Upatnieks, Juris: Wavefront Reconstruction with Diffused Illumination and Three-Dimensional Objects. J. Opt. Soc. Am., vol. 54, no. 11, Nov. 1964, pp. 1295-1301.

11. Liu, B.; and Gallagher, N. C.: Convergence of a Spectrum Shaping Algorithm. Appl. Opt., vol. 13, no. 11, Nov. 1974, pp. 2470-2471.

12. Enloe, L. H.; Murphy, J. A.; and Rubenstein, C. B.: Hologram Transmission Via Television. Bell Syst. Tech. J., vol. 45, no. 2, Feb. 1966, pp. 335-339.

13. Enloe, L. H.; Jakes, W. C., Jr.; and Rubenstein, C. B.: Hologram Heterodyne Scanners. Bell Syst. Tech. J., vol. 47, no. 9, Nov. 1968, pp. 1875-1882.

14. Larsen, Arthur B.: A Heterodyne Scanning System for Hologram Transmission. Bell Syst. Tech. J., vol. 48, no. 7, Sept. 1969, pp. 2507-2527.

15. Yariv, Amnon: Introduction to Optical Electronics. Holt, Rinehart, and Winston, Inc., 1971, p. 40.

16. Macovski, A.: Spatial and Temporal Analysis of Scanned Systems. Appl. Opt., vol. 9, no. 8, Aug. 1970, pp. 1906-1910.

17. Abramowitz, Milton; and Stegun, Irene A.: Handbook of Mathematical Functions with Formulas, Graphs, and Mathematical Tables. Dover Publications, Inc., 1964, p. 361.

18. Reference Data for Radio Engineers. Fifth ed. Howard W. Sams and Co., Inc., 1972, pp. 16-42 to 16-44.

19. Leighty, R. D., ed.: Data Extraction and Classification from Film, Proceedings. Society of Photo-Optical Instrumentation Engineers, Vol. 117, 1977.

20. Lehmann, M.: Investigation of a Photodichroic Material for Holographic Storage and Recovery. Final Technical Report, Mar. 1972-Apr. 1977, Stanford Research Inst., 1977. (AD-A041597.)

21. Petit, R. H.; Ferre, J.; and Badoz, J.: Observation of the Twin-Walls Movement in $KNiF_5$ by Dichroism. Magnetism and Magnetic Materials - 1974. AIP Conference Proceedings, No. 24, C. D. Graham, Jr., G. H. Lander, and J. J. Rhyne, eds., American Institute of Physics, 1975, pp. 184-185.

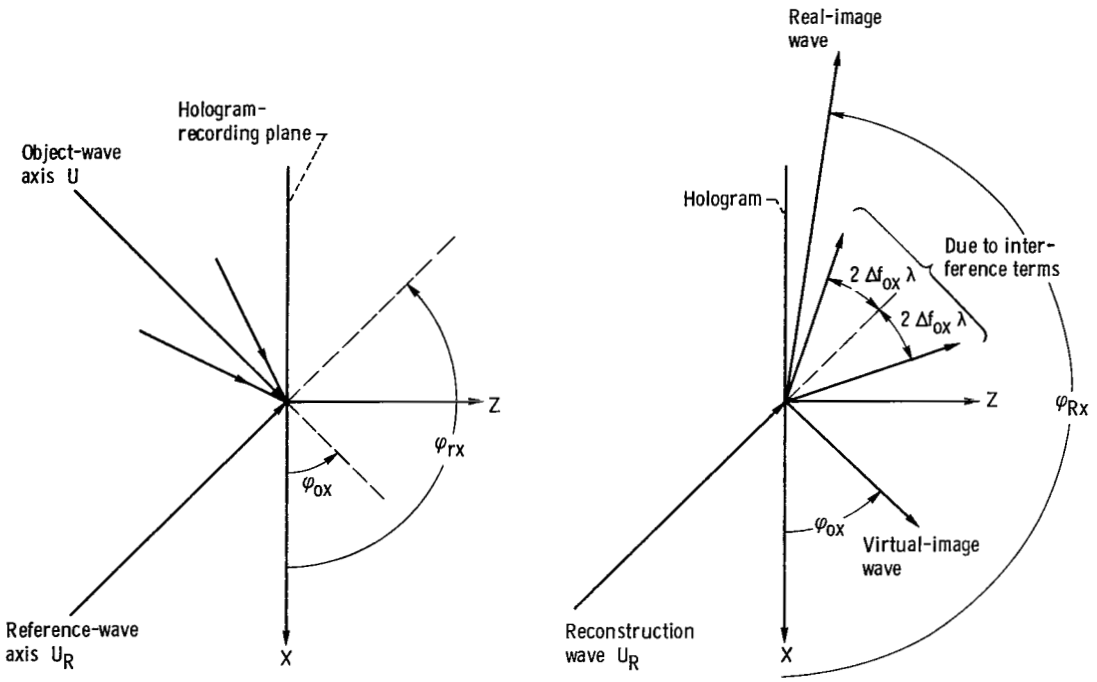

(a) Schematic of hologram-recording process in x, z-plane. (Reference wave has negligible spread.)

(b) Schematic of reconstruction process in x, z-plane. (Only axes of image waves are shown.)

Figure 1. - Schematics of hologram-recording and reconstruction processes.

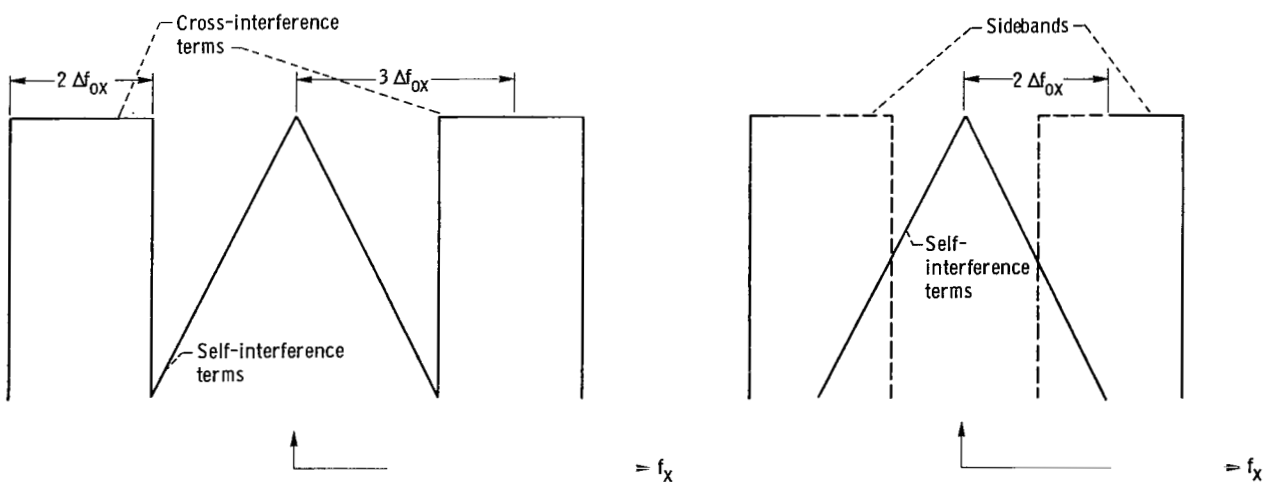

(a) Recorded with off-axis reference wave.

(b) Recorded with off-axis reference wave when single sideband will be retained.

Figure 2. - One-dimensional spatial-frequency spectra of hologram.

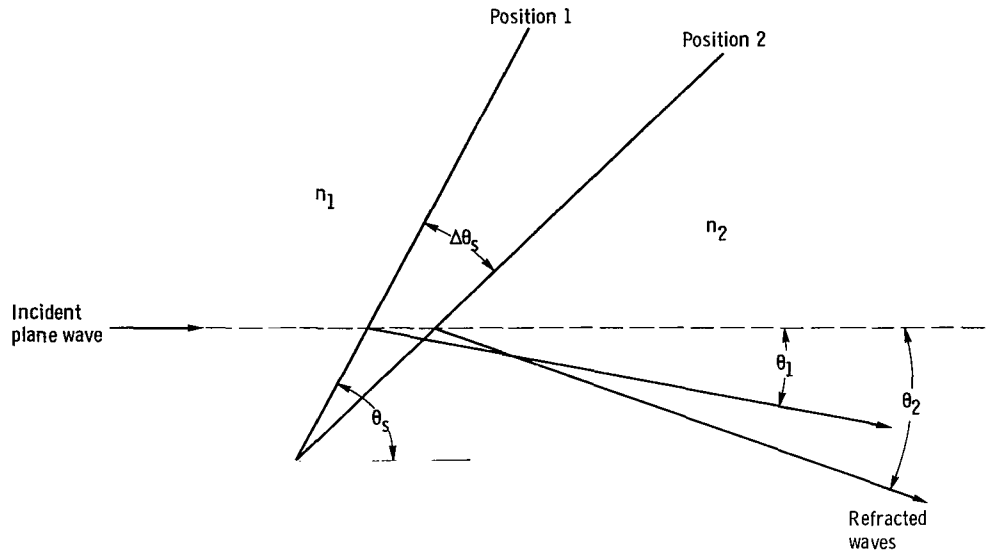

Figure 3. - Double exposure of refraction from rotating shock wave.

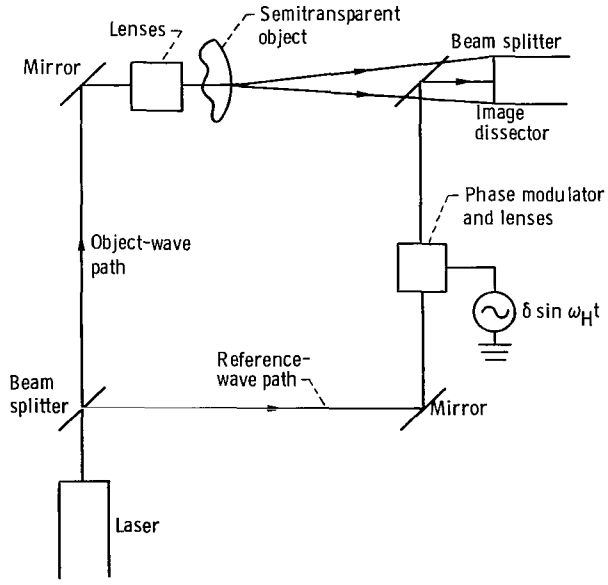

Figure 4. - Arrangement for recording low-resolution hologram of transparency.

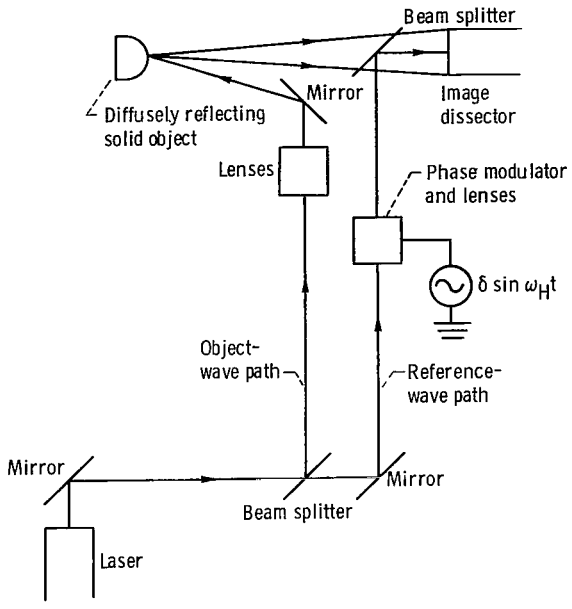

Figure 5. - Arrangement for recording low-resolution hologram of solid object.

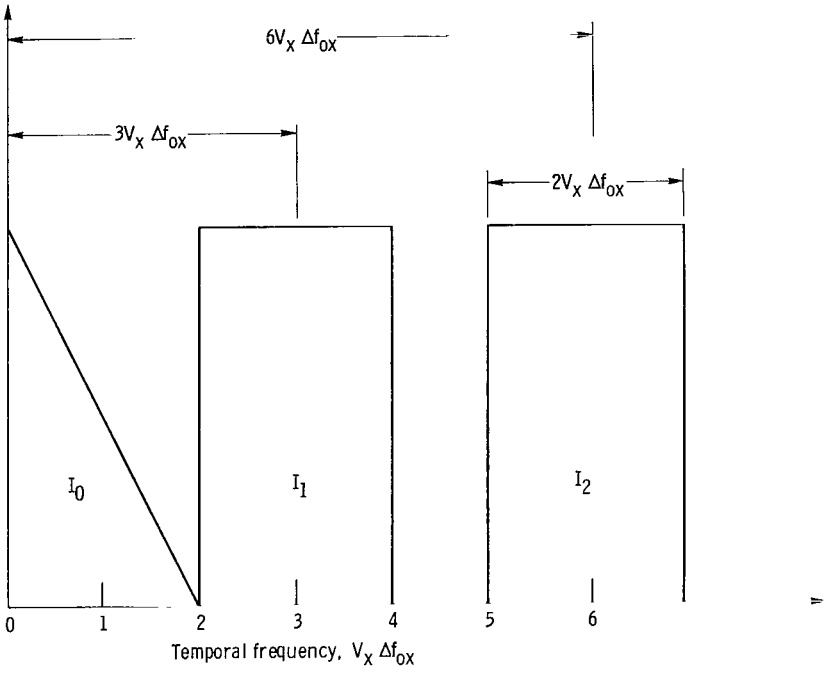

Figure 6. - Spectrum of nonoverlapping bands for unqualified separation of signals for $f_H = 3V_x \Delta f_{ox}$.

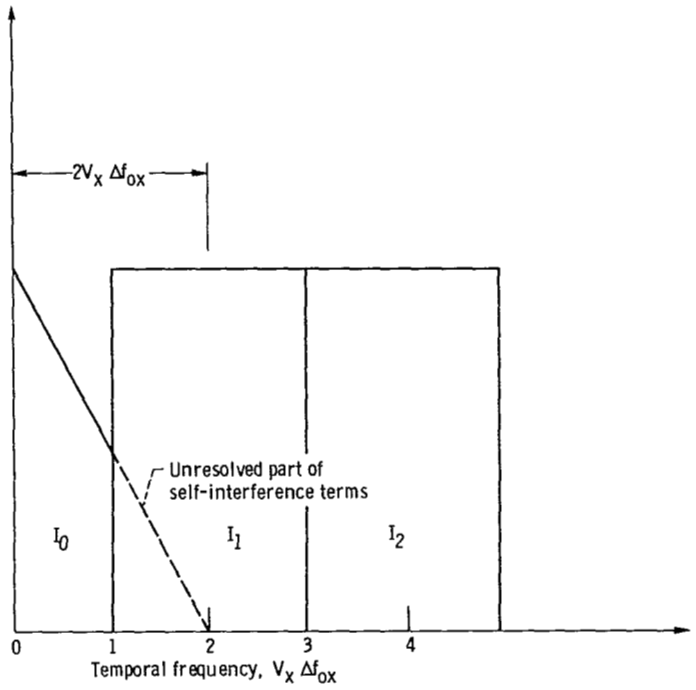

Figure 7. - Spectrum of nonoverlapping bands when frequencies exceeding maximum object-wave frequency are not resolved and $f_H = 2V_x\ \Delta f_{ox}$.

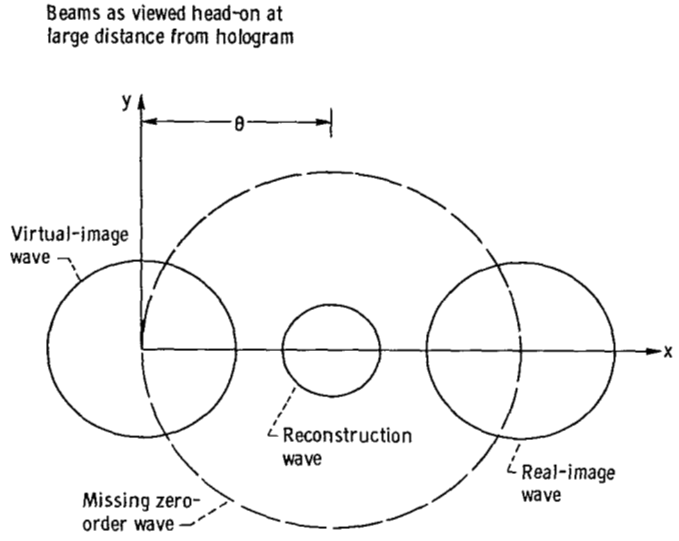

Figure 8. - Reconstruction of hologram recorded by heterodyne method.

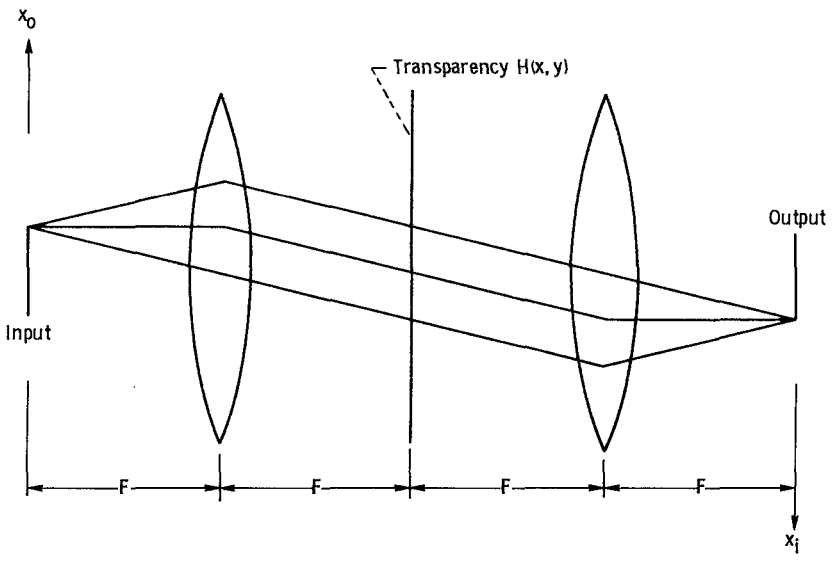

Figure 9. - Spatial-filtering operation using pair of lenses.

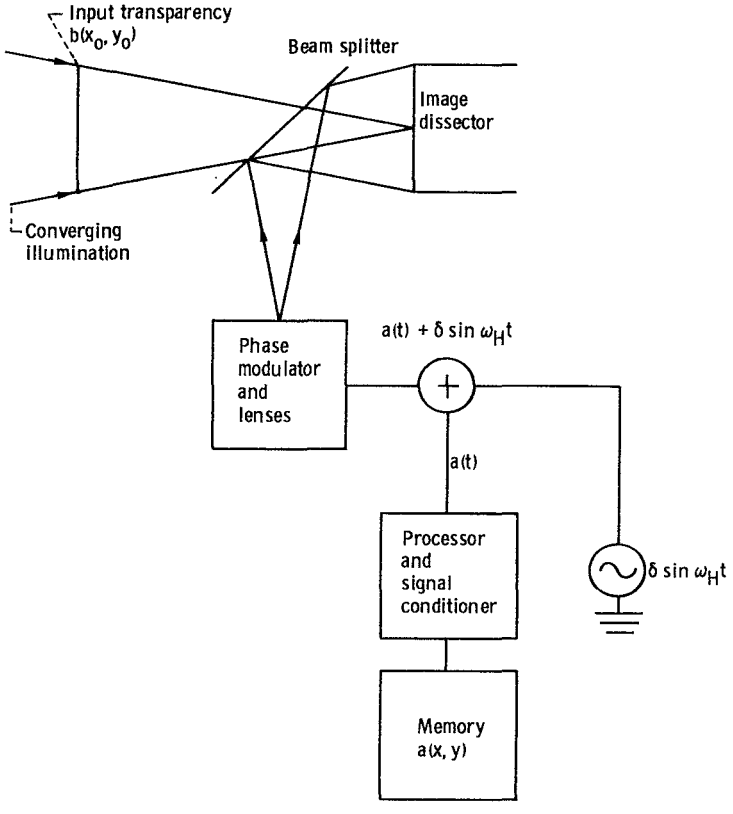

Figure 10. - Spatial-filtering operation using lenseless transform and heterodyne processing.

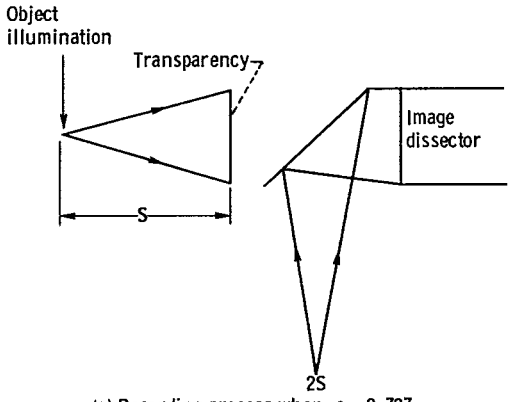

(a) Recording process when a = 0.707.

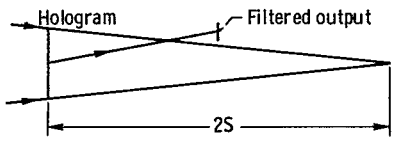

(b) Reconstruction process. (Only real-image output shown.)

Figure 11. - Filtered output in real image with virtual image at infinity.

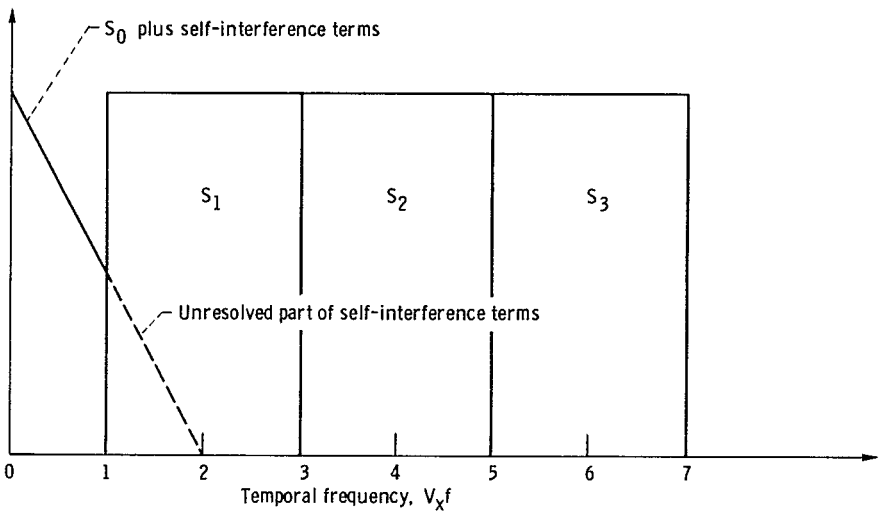

Figure 12. - Spectrum of bands in pulsed-laser case when f is maximum spatial frequency resolved by polarization-sensitive detector.

1. Report No.	2. Government Accession No.	3. Recipient's Catalog No.
NASA TP-1444		

4. Title and Subtitle	5. Report Date
SIMULATED ELECTRONIC HETERODYNE RECORDING AND PROCESSING OF PULSED-LASER HOLOGRAMS	April 1979
	6. Performing Organization Code
7. Author(s)	8. Performing Organization Report No.
Arthur J. Decker	E-9813
	10. Work Unit No.
9. Performing Organization Name and Address	505-04
National Aeronautics and Space Administration Lewis Research Center Cleveland, Ohio 44135	11. Contract or Grant No.
	13. Type of Report and Period Covered
12. Sponsoring Agency Name and Address	Technical Paper
National Aeronautics and Space Administration Washington, D.C. 20546	14. Sponsoring Agency Code

15. Supplementary Notes

16. Abstract

A method is proposed for the electronic recording of pulsed-laser holograms. The polarization sensitivity of each resolution element of the detector is controlled independently to add an arbitrary phase to the image waves. This method can be used to simulate heterodyne recording and to process three-dimensional optical images. The method is based on a similar method for heterodyne recording and processing of continuous-wave holograms.

17. Key Words (Suggested by Author(s))	18. Distribution Statement
Holography; Optical heterodyning; Spatial filtering; Electronic recording systems; Television equipment; Flow visualization	Unclassified - unlimited STAR Category 16

19. Security Classif. (of this report)	20. Security Classif. (of this page)	21. No. of Pages	22. Price*
Unclassified	Unclassified	39	A03

* For sale by the National Technical Information Service, Springfield, Virginia 22161

NASA-Langley, 1979

10 1 1U,D, 030979 S00903DS
DEPT OF THE AIR FORCE
AF WEAPONS LABORATORY
ATTN: TECHNICAL LIBRARY (SUL)
KIRTLAND AFB NM 87117